Int. J. Solids Structures Vol. 16, pp. 451–463
© Pergamon Press Ltd., 1980. Printed in Great Britain
0020-7683/80/0501-0451/$02.00/0

AN INITIAL FLEXURAL FAILURE ANALYSIS OF SYMMETRICALLY LAMINATED CROSS-PLY RECTANGULAR PLATES

G. J. TURVEY
Department of Engineering, University of Lancaster, Lancaster, England

(*Received* 20 *March* 1979; *in revised form* 20 *July* 1979)

Abstract—It is shown that by combining the exact (Navier) solution of the specially orthotropic plate equilibrium equations with the Tsai–Hill failure criterion the initial failure analysis of fibre reinforced laminated plates may be transformed into an optimisation problem. A simple trial and error procedure is used to locate and evaluate the maximum value of an initial failure function from which the initial failure load and the corresponding plate deflections may be evaluated. This approach is used to provide design data for the initial failure condition in GFRP and CFRP simply supported, rectangular plates subjected to uniform, uniform square patch and hydrostatic (linearly varying) load distributions.

NOTATION

a	plate side length (x co-ordinate direction)
A_{mn}	Fourier deflection coefficient
b	plate side length (y co-ordinate direction)
c, d	patch load dimensions
$D_{11}, D_{12}, D_{22}, D_{66}$	plate flexural rigidities
$D_T (= E_T h^3 (1 - \nu_{LT}\nu_{TL})^{-1}/12)$	plate flexural rigidity
e_1, e_2, e_{12}	strains referred to lamina principal axes
e_x, e_y, e_{xy}	strains referred to plate principal axes
E_L, E_T	longitudinal and transverse elastic moduli
G_{LT}	shear modulus
h	plate thickness
k	lamina number
k_x, k_y, k_{xy}	plate curvatures and twist
N_L	number of laminae in the plate
q, q_0	lateral pressure
$\bar{q} (= q_0 a^2 s_1^{-1} h^{-2})$	dimensionless initial failure load
q_{mn}	Fourier load coefficient
$R (= ba^{-1})$	plate aspect ratio
s_1, s_2, s_{12}	stresses referred to lamina principal axes
s_L, s_{T_c}, s_{LT}	lamina strengths (longitudinal, transverse and shear)
t	lamina thickness
w	plate deflection
$\bar{w} (= wD_T a^{-2} s_1^{-1} h^{-2})$	dimensionless deflection
$\bar{w}_c$	dimensionless plate centre deflection
x, y, z	Cartesian co-ordinate directions
x_1, y_1	co-ordinates of patch centre
z_{k-1}, z_k	positions of kth lamina's surfaces (see Fig. 1)
ξ_k	vector defining the position of the initial failure surface relative to the plate reference surface for the kth lamina
ϕ_k, ϕ_{1k}	initial and modified failure functions for the kth lamina
$(\phi_{1k})_{max}, (\phi_{1k})^*_{max}$	maximum value of ϕ_{1k} for the kth and for all of the laminae
ν_{LT}, ν_{TL}	Poisson's ratios
$(\dot{}), (\,)'$	partial differentiation with respect to x and y

1. INTRODUCTION

Despite continuing research effort, satisfactory analytical techniques are not yet available for tracing the response of fibre reinforced, laminated structural elements up to collapse. This situation persists largely because of the complex nature of failure in composite materials—several modes of failure are possible and the possibility of interaction between them is not precluded. As yet no thoroughly adequate failure criteria have been put forward. Until this impasse is overcome, the design of laminated structural elements is likely to be based on the onset of *initial failure in an individual lamina of the laminate*, even though such a criterion may be very conservative from the strength standpoint[1]. Thus, initial failure analyses may be regarded as a useful means of generating design data for laminated structures.

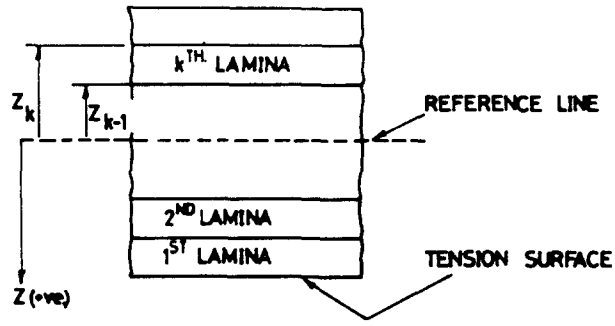

Fig. 1. Section through the laminated plate showing the lamina reference system.

The present paper is concerned with examining the initial failure of laminated rectangular plates. Hitherto, most initial failure analyses have concentrated on in-plane rather than out-of-plane loading states, probably because the former are more dominant in the situations where laminated structural elements enjoy their greatest potential, i.e. in aircraft structures. However, laminated structural elements are beginning to be used in other situations for which flexure is the dominant load supporting action. It is for these latter situations that the results presented herein may be expected to be of use.

Attention is deliberately focussed on symmetric, cross-ply lay-ups, because the resulting laminates/plates exhibit specially orthotropic properties in flexure. This feature, apart from being of great practical significance, allows virtually exact initial failure loads and deflections to be evaluated for several practically important lateral pressure distributions. However, as far as the present analysis is concerned, this degree of exactitude is achieved only at the price of restricting the applicability of the computed results to plates which are simply supported on all four sides (the severity of the restriction on the plate boundary conditions can be eased by utilising the Levy rather than the Navier solution to the plate equilibrium equation).

The computer program developed for the exact, initial flexural failure analysis of simply supported, rectangular plates has been used to carry out a reasonably comprehensive parameter study. The following parameters have been included: the degree of orthotropy (a characteristic of the material type), the lateral pressure distribution, the plate aspect ratio and the number of laminae in the laminate. All of the computed initial failure loads and associated plate centre deflections for the complete parameter range are presented in dimensionless, graphical form to facilitate direct design application.

2. LAMINA DATA, LAY-UP DETAILS AND PLATE RIGIDITIES

In this paper attention is restricted to the most common high modulus, fibre reinforced materials, viz GFRP (Glass Fibre Reinforced Plastic) and CFRP (Carbon Fibre Reinforced Plastic). The stiffness and strength ratios for individual laminae of these two materials have been taken from Refs. [2 and 3] and are given in Table 1.

Only symmetric, cross-ply lay-ups are considered; thus, each plate consists of an odd number of identical laminae, the fibre directions of which are alternately aligned with and normal to the plate x-axis.

If, relative to the plate mid-plane, the outermost laminae are chosen to have their fibre directions aligned with the x-axis, then the following simple formulae[2] may be used to evaluate the plate rigidities,

$$
\begin{aligned}
D_{11} &= \alpha E^{*}_{T} h^3 \{(\alpha^{-1} - 1)P + 1\}/12 \\
D_{12} &= \nu_{LT} E^{*}_{T} h^3/12 \\
D_{22} &= \alpha E^{*}_{T} h^3 \{(1 - \alpha^{-1})P + \alpha^{-1}\}/12 \\
D_{66} &= \beta E^{*}_{T} h^3/12
\end{aligned} \tag{1}
$$

Table 1. Stiffness and strength data for GFRP and CFRP unidirectional laminae.

(a) Stiffness data			
Material	$E_L E_T^{-1}$	$G_{LT} E_T^{-1}$	ν_{LT}
GFRP	3.00	0.48	0.25
CFRP	9.40	0.36	0.30
(b) Strength data			
Material	$s_L s_{T_t}^{-1}$	$s_T s_{T_t}^{-1}$	$s_{LT} s_{T_t}^{-1}$
GFRP	37.50	4.00	1.50
CFRP	17.85	2.64	1.43

in which

$$\alpha = E_L E_T^{-1},\ E_T^* = E_T(1 - \nu_{LT}\nu_{TL})^{-1}$$

$$\beta = G_{LT} E_T^{-1}(1 - \nu_{LT}\nu_{TL})$$

$$P = (1+M)^{-3} + M(N_L - 3)\{M(N_L - 1) + 2(N_L + 1)\} \times (N_L^2 - 1)(1+M)^{-3}$$

and

$$M = \left(\sum_{k=\text{odd}} t_k\right)\left(\sum_{k=\text{even}} t_k\right)^{-1}.$$

3. ANALYSIS

An initial flexural failure analysis may be regarded as the means by which the magnitude of the lateral pressure is determined such that equilibrium is maintained at all points throughout the structure and yet a state of incipient failure exists at one or more of these points. Thus, two aspects are embodied in such an analysis: the maintenance of equilibrium and the satisfaction of the failure criterion. Each of these will be treated separately, and then it will be demonstrated that their subsequent combination allows the problem to be transformed into an optimisation problem, namely, that of seeking the maximum value of an initial failure function. Once this maximum value has been determined the required initial failure load and associated plate centre deflection may be readily calculated.

(a) *Solution of the plate equilibrium equation*

Restricting the analysis to symmetric, cross-ply lay-ups ensures that the plate exhibits specially orthotropic flexural properties. Furthermore, if initial failure is assumed to occur within the small deflection regime, then a single, fourth order, partial differential equation is sufficient to describe plate equilibrium[4],

$$D_{11} w'''' + 2(D_{12} + 2D_{66}) w''' + D_{22} w'''' = q. \tag{2}$$

As the plate is simply supported along all four sides, the deflection surface and the lateral pressure distribution may both be expressed in classical Navier double series form,

$$w = \sum_{m=1}^{\infty} \sum_{n=1}^{\infty} A_{mn} \sin(m\pi x/a) \sin(n\pi y/b) \tag{3}$$

and

$$q = \sum_{m=1}^{\infty} \sum_{n=1}^{\infty} q_{mn} \sin(m\pi x/a) \sin(n\pi y/b). \tag{4}$$

Now substituting eqns (3) and (4) into eqn (2), the coefficients, A_{mn}, may be defined in terms of the known coefficients, q_{mn}, as,

$$A_{mn} = q_{mn} D_{mn}^{-1} \tag{5}$$

in which

$$D_{mn} = D_{11}(m\pi/a)^4 + 2(D_{12} + 2D_{66})(m\pi/a)^2(n\pi/b)^2 + D_{22}(n\pi/b)^4.$$

Substituting eqn (5) into eqn (3) allows the deflection field to be properly defined throughout the plate. This deflection field is readily differentiated to yield the plate curvatures and twist, which may then be used to determine the strains (relative to plate axes) at any point within the plate thickness as follows,

$$\begin{bmatrix} e_x \\ e_y \\ e_{xy} \end{bmatrix} = z \begin{bmatrix} k_x \\ k_y \\ k_{xy} \end{bmatrix} = -z \begin{bmatrix} w'' \\ w'' \\ 2w'' \end{bmatrix}. \tag{6}$$

The principal strains in the kth lamina may then be determined by employing the following strain transformation relationship,

$$\begin{bmatrix} e_1 \\ e_2 \\ e_{12} \end{bmatrix}_k = \begin{bmatrix} c^2 & s^2 & cs \\ s^2 & c^2 & -cs \\ -2cs & 2cs & (c^2 - s^2) \end{bmatrix} \begin{bmatrix} e_x \\ e_y \\ e_{xy} \end{bmatrix}_k \tag{7}$$

in which $c = \cos\theta$ and $s = \sin\theta$ and θ is the fibre orientation angle of the kth lamina.

On substituting eqn (7) into the lamina stress–strain relationship, the stresses (relative to lamina principal axes) in the kth lamina are given by,

$$\begin{bmatrix} s_1 \\ s_2 \\ s_{12} \end{bmatrix}_k = E_T^* \begin{bmatrix} \alpha & \nu_{LT} & 0 \\ \nu_{LT} & 1 & 0 \\ 0 & 0 & \beta \end{bmatrix} \begin{bmatrix} e_1 \\ e_2 \\ e_{12} \end{bmatrix}_k \tag{8}$$

Equations (6)–(8) may now be combined to enable the lamina stress components in the kth layer to be re-expressed as,

$$\begin{bmatrix} s_1 \\ s_2 \\ s_{12} \end{bmatrix}_k = -z_1 E_T^* \begin{bmatrix} a_{11} & a_{12} & a_{13} \\ a_{21} & a_{22} & a_{23} \\ a_{31} & a_{32} & a_{33} \end{bmatrix} \begin{bmatrix} w'' \\ w'' \\ 2w'' \end{bmatrix} \tag{9}$$

in which

$$a_{11} = \alpha c^2 + \nu_{LT} s^2$$
$$a_{12} = \alpha s^2 + \nu_{LT} c^2$$
$$a_{13} = (\alpha - \nu_{LT})cs$$
$$a_{21} = (\nu_{LT} c^2 + s^2)$$
$$a_{22} = (\nu_{LT} s^2 + c^2)$$
$$a_{23} = (\nu_{LT} - 1)cs$$
$$a_{31} = -2\beta cs$$
$$a_{32} = -a_{31}$$
$$a_{33} = \beta(c^2 - s^2)$$

and z_l varies from z_{k-1} to z_k (see Fig. 1). (*N.B.* The expressions for $a_{11}, \ldots, a_{33}$ may be further simplified for the cross-ply lay-ups considered herein, since $c = 1$ and $s = 0$ for odd-numbered and $c = 0$ and $s = 1$ for even-numbered laminae.)

(b) *Lamina failure criterion*

There are a number of lamina failure criteria which may be employed in the initial flexural failure analysis of a laminated plate. Tsai[5] shows that the Tsai–Hill failure criterion gives good correlation with experiment for GFRP laminates subjected to in-plane loading configurations and it has therefore been selected for incorporation into the present analysis. This criterion takes the following form,

$$\gamma^2(s_1^2 - s_1 s_2) + \delta^2 s_2^2 + \epsilon^2 s_{12}^2 = s_{Tt}^2 \tag{10}$$

in which

$$\gamma = s_{T_t} s_L^{-1}$$

$$\delta = \begin{cases} 1 & \text{when } s_2 \text{ is tensile} \\ s_{T_t} s_{T_c}^{-1} & \text{when } s_2 \text{ is compressive} \end{cases}$$

$$\epsilon = s_{T_t} s_{LT}^{-1}.$$

(c) *Laminate initial failure criterion*

On substituting eqn (9) into eqn (10) and setting $z_l = \xi_k$, two surfaces are defined, which are unique to the kth lamina. The distance of these surfaces, one of which is shown in Fig. 2, from the laminate mid-plane is given by,

$$\xi_k = \pm s_{T_t} E_T^{*-1} \phi_k^{-(1/2)} \tag{11}$$

in which

$$\phi_k = f(w'^2, w''^2, w'^2, w'w'', w'w', w''w').$$

These two surfaces are not equidistant from the laminate midplane because the value of ϕ_k associated with the positive sign differs from that associated with the negative sign—a feature which is directly attributable to the difference in the lamina compressive and tensile strengths. In general, therefore, only one of any symmetric pair of laminae may reach a state of incipient failure—the one in which the lamina transverse stress is tensile.

For a state of incipient failure to exist in the kth lamina, ξ_k must assume its minimum value, i.e. $(\xi_k)_{\min} = z_k$ at one or more points (see Fig. 2). This implies that $\phi_k = (\phi_k)_{\max}$, so that,

$$z_k = \pm s_{T_t} E_T^{*-1} (\phi_k)_{\max}^{-(1/2)}. \tag{12}$$

But z_k may be expressed in terms of the plate thickness, the thickness of an individual lamina and the lamina number as follows,

$$z_k = \frac{1}{2} h - (k-1)t \tag{13}$$

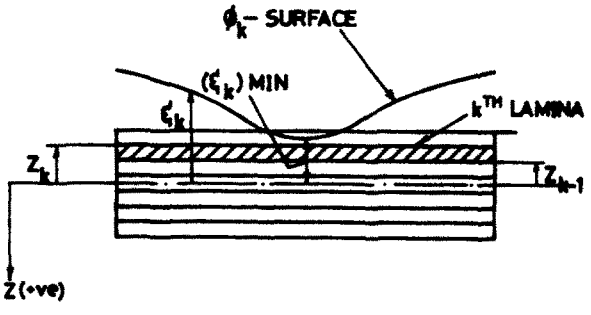

Fig. 2. Section through the laminated plate showing the kth lamina's initial failure surface.

in which

$$k = 1 \rightarrow N_L.$$

Substituting eqn (13) into eqn (12) and re-arranging gives,

$$\frac{1}{2}h = \pm s_{T_t} E_T^{*-1} (\phi_{1k})_{\max}^{-(1/2)} \tag{14}$$

in which

$$(\phi_{1k})_{\max} = (\phi_k)_{\max}\{1 - 2(k-1)N_L^{-1}\}^2.$$

Thus, the initial flexural failure analysis reduces to the evaluation of $(\phi_{1k})_{\max}$ for each of the laminae. The maximum of these, i.e. $(\phi_{1k})^*_{\max}$ is the required solution to the problem and the required initial failure load and associated plate deflections may be obtained by simple scaling as follows,

$$\bar{q} = (\bar{\phi}_{1k})_{\max}^{*-(1/2)}/6 \tag{15}$$

in which

$$(\phi_{1k})_{\max}^{*-(1/2)} = q_0^{-1} D_T a^{-2} (\bar{\phi}_{1k})_{\max}^{*-(1/2)}$$

and

$$\bar{w} = \bar{q}w \tag{16}$$

(d) *Load distributions*

The present analysis is unrestricted in the type of load distribution that may be considered. However, only three such distributions will be considered here, viz. uniform, patch and hydrostatic (linearly varying). The forms of the q_{mn} terms in eqn (4) appropriate to each of these are given below as:

(i) *Uniformly distributed load*

$$q_{mn} = 16\pi^{-2} m^{-1} n^{-1} q_0 \tag{17}$$

in which

$$m = n = 1, 3, 5, \ldots \ .$$

(ii) Uniformly distributed rectangular patch load

$$q_{mn} = 16\pi^{-2} m^{-1} n^{-1} \sin(m\pi x_1/a) \sin(n\pi y_1/b) \sin\left(\frac{1}{2} m\pi c/a\right) \sin\left(\frac{1}{2} n\pi d/b\right) q_o \tag{18}$$

in which

$$m = n = 1, 3, 5, \ldots, \tag{18}$$

x_1 is the x co-ordinate of the patch centre,

y_1 is the y co-ordinate of the path centre,

and c and d are the patch dimensions relative to the x and y co-ordinate directions respectively.

(iii) *Hydrostatically (linearly varying) distributed load*

$$q_{mn} = -8\pi^{-2}m^{-1}n^{-1}\cos(n\pi)q_0 \tag{19}$$

in which

$$m = 1,3,5,\ldots \quad \text{and} \quad n = 1,2,3,\ldots \; . \tag{19}$$

(e) *Evaluation of* $(\phi_{1k})^*_{max}$

A simple trial and error procedure is employed to locate and evaluate $(\phi_{1k})_{max}$ for each lamina. Basically, ϕ_{1k} is evaluated at each node of a rectangular or square grid extending over the whole of the lamina. By comparing the ϕ_{1k} values at each node with one another, either $(\phi_{1k})_{max}$ and its location are determined directly, or a region(s) which contains $(\phi_{1k})_{max}$ is isolated for reanalysis using a finer mesh. Repeating this procedure for each of the laminae in the plate enables $(\phi_{1k})^*_{max}$ to be located and evaluated to any desired degree of accuracy.

Because of certain features of the problem under consideration—notably the plate boundary conditions, the type of anisotropy and the form of the failure criterion—it was found

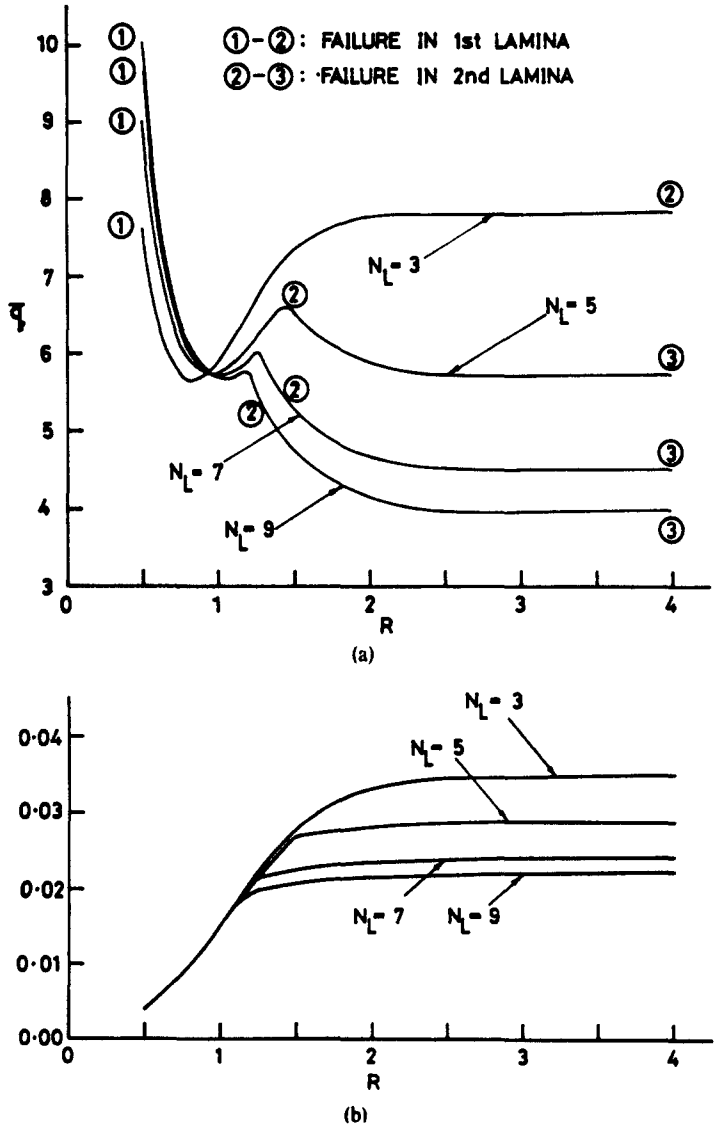

Fig. 3. Uniformly loaded, simply supported GFRP cross-ply plate. (a) Initial failure load vs plate aspect ratio. (b) Corresponding plate centre deflection vs plate aspect ratio.

that initial failure always occurred along the plate centre-line parallel to the y-axis (at one or two locations) in the outermost our next outermost lamina on the tension side of the plate midplane, i.e. in the laminae $k = 1$ or 2 shown on Fig. 1. Thus, once this pattern was recognised, it was no longer necessary to implement in full the trial and error procedure for locating $(\phi_{1k})_{max}$ and the computational effort was considerably reduced.

4. COMPUTED INITIAL FAILURE LOADS AND DEFLECTIONS

Two sets of results have been computed—initial failure loads and corresponding plate centre deflections—for each of the two material types and three lateral pressure distributions considered. These results are presented in dimensionless graphical form in order to facilitate direct design application.

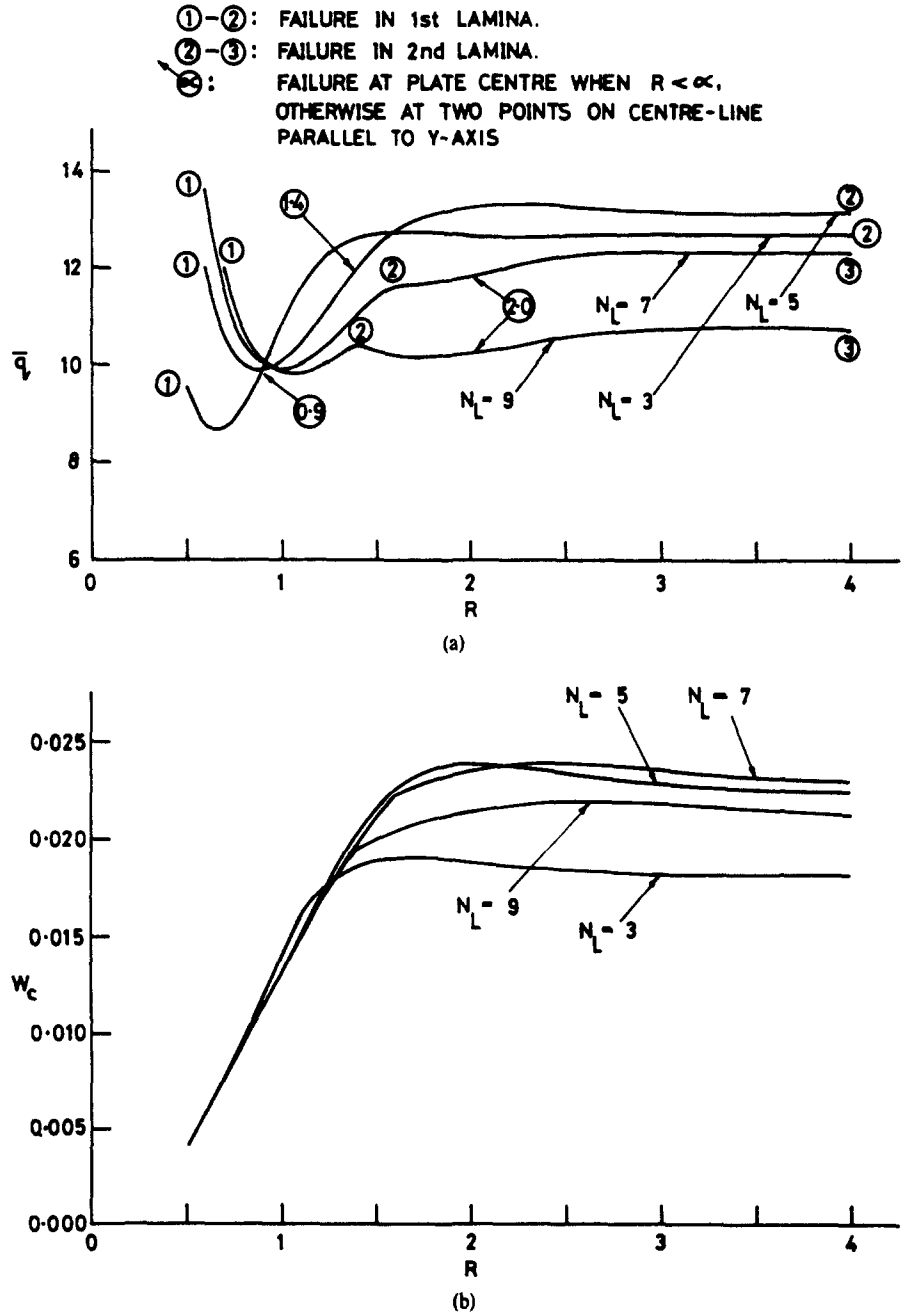

Fig. 4. Uniformly loaded, simply supported CFRP cross-ply plate. (a) Initial failure load vs plate aspect ratio. (b) Corresponding plate centre deflection vs plate aspect ratio.

The initial failure loads and corresponding plate centre deflections for uniformly loaded GFRP and CFRP plates are depicted in Figs. 3 and 4 respectively. It is evident that the GFRP plate initial failure loads (see Fig. 3a) are sensibly constant once the plate aspect ratio, R, exceeds a value of approximately two and, moreover, these failure loads decrease as the number of laminae in the plate increases—the initial failure load drops by about 50% when the number of laminae, N_L, increases from 3 to 9. Another important feature of the curves shown in Fig. 3(a) is the presence of local minima and/or maxima—the former all occurring at an aspect ratio of approximately one. For uniformly loaded GFRP plates failure was always observed to initiate at the plate centre in the first or second lamina ($k = 1$ ro 2). Each of the curves in Fig. 3(a) is marked to show the range of aspect ratios over which failure initiates in each of these two laminae. It is evident that failure initiates in the first lamina at low values of R and that the second lamina fails first at higher values, provided $N_L > 3$.

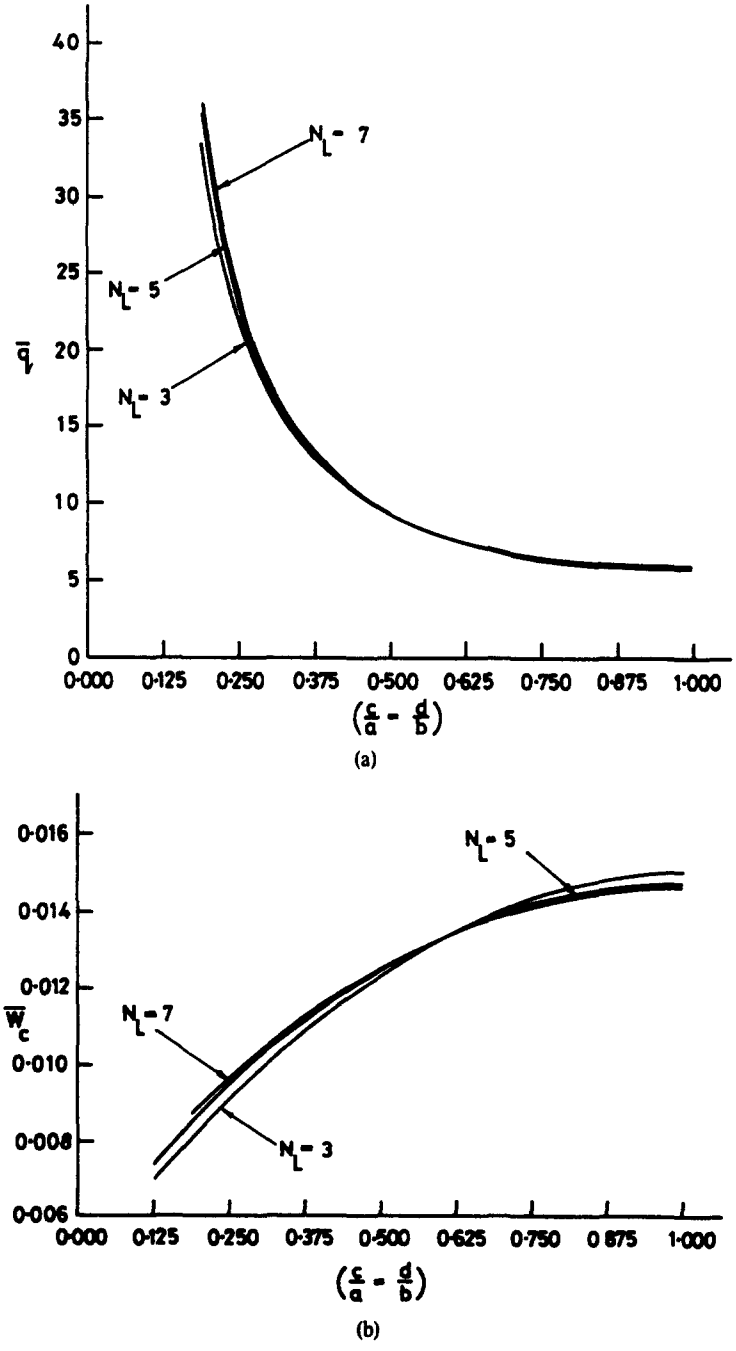

Fig. 5. Square, simply supported GFRP cross-ply plate subjected to a uniform, square patch load at its centre. (a) Initial failure load vs patch size. (b) Corresponding plate centre deflection vs patch size.

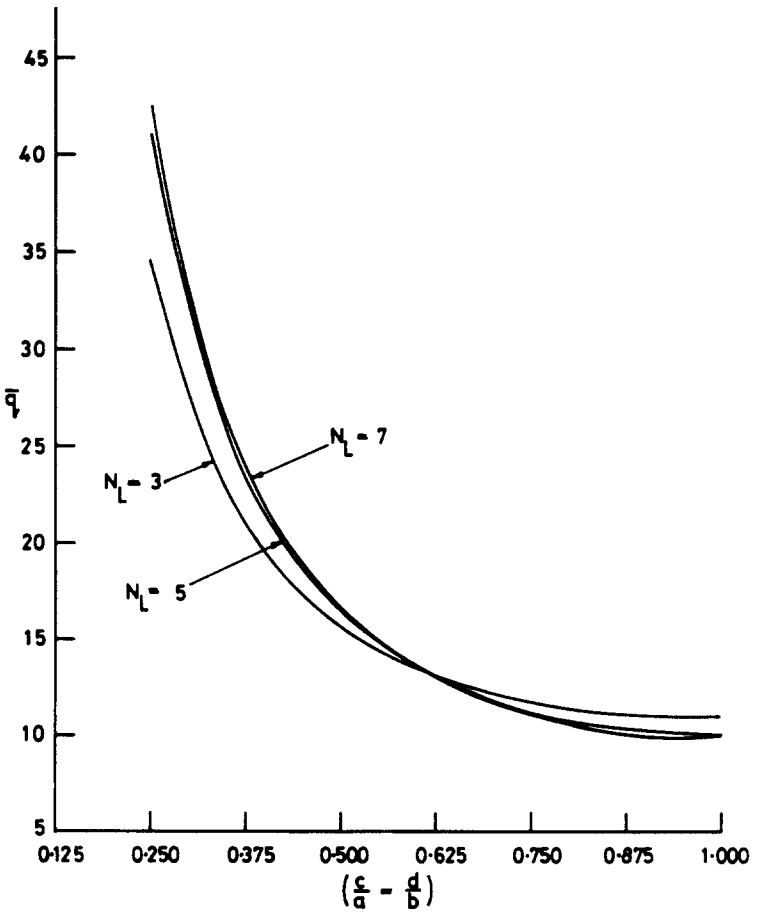

(a)

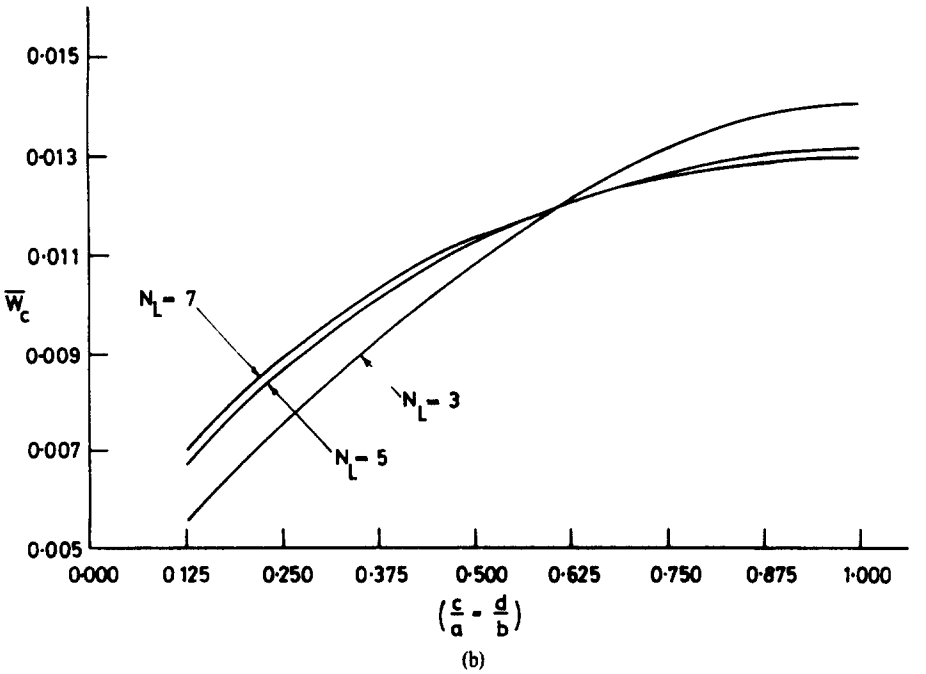

(b)

Fig. 6. Square, simply supported CFRP cross-ply plate subjected to a uniform, square patch load at its centre. (a) Initial failure load vs patch size. (b) Corresponding plate centre deflection vs patch size.

The initial failure load curves for CFRP plates are presented in Fig. 4(a). They also exhibit local minima when $R \doteq 1$ and tend to constant values (i.e. exhibit aspect ratio independence) when $R > 2.5$. However, in contrast to GFRP plates, the initial failure loads of high aspect ratio CFRP plates do not necessarily decrease as the number of laminae increases, e.g. the curve for $N_L = 5$ lies above that for $N_L = 3$ and that for $N_L = 7$ lies only marginally below it. Each of the curves of Fig. 4(a) is marked to show the range of aspect ratios over which failure initiates in the first and second laminae. Furthermore, as failure does not always initiate at the plate centre, the curves are additionally marked to show the range of aspect ratios for which symmetric, two-point centre-line failure applies.

The plate centre deflections corresponding to the initial failure loads of Figs. 3(a) and 4(a) are presented in Figs. 3(b) and 4(b) respectively. For uniformly loaded, GFRP plates (see Fig. 3b) the plate centre deflections are practically independent of N_L provided $R \leq 1.1$; otherwise

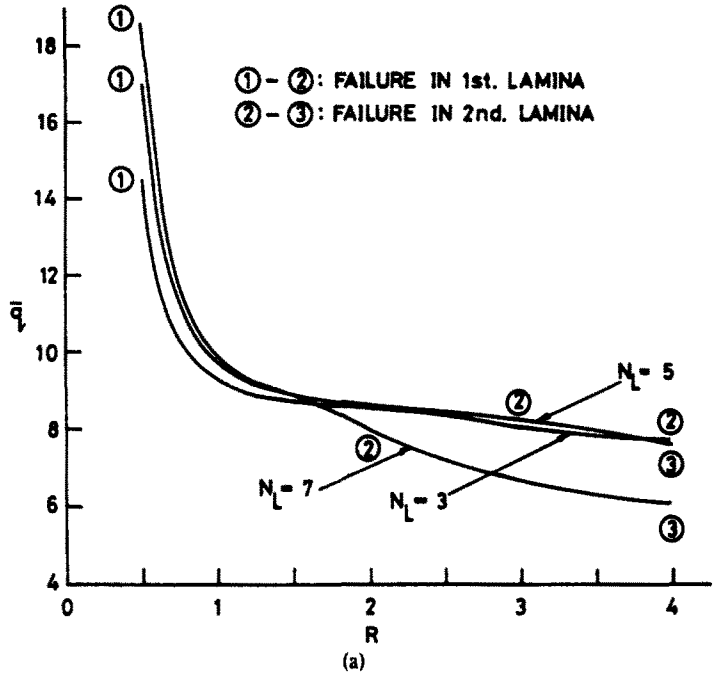

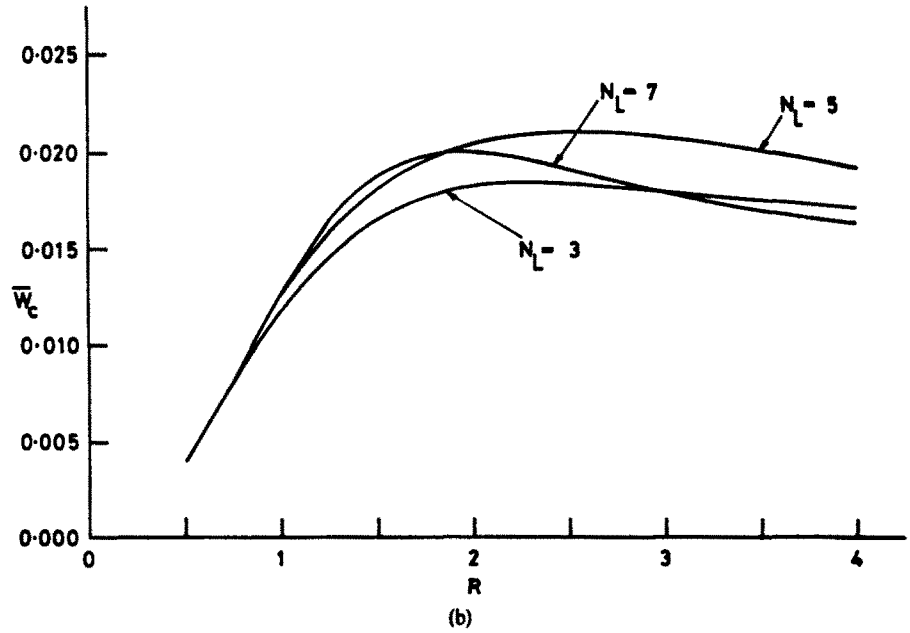

Fig. 7. Hydrostatically loaded, simply supported GFRP cross-ply plate. (a) Initial failure load vs plate aspect ratio. (b) Corresponding plate centre deflection vs plate aspect ratio.

they decrease as N_L increases. Furthermore, when $R > 2$ the deflections are sensibly constant, i.e. they are aspect ratio independent. Similar features are present in the deflection curves for uniformly loaded, CFRP plates shown in Fig. 4(b)—the notable exception being that the central deflection tends, if anything, to increase rather than decrease with N_L when $R \geq 1.1$.

From the design standpoint, the uniformly loaded, GFRP and CFRP plate results of Figs. 3 and 4 suggest (particularly where serviceability limits on deflections are of no consequence) that maximum plate strength may be achieved by minimising the number of laminae in the plate when $R > 1$ and maximising this number when $R < 1$.

Results for square, GFRP and CFRP plates subjected to uniform, square patch loads of varying size at their centres are presented in Figs. 5 and 6. It is evident that the initial failure loads for both material types decrease rapidly as the patch size increases (see Figs. 5a and 6a). Figures 5(b) and 6(b) show that the inverse situation applies for the corresponding plate centre deflections. These figures clearly demonstrate that the number of laminae has very little influence on either the initial failure load or the corresponding plate centre deflection. This latter feature is thought to be primarily due to the choice of a unit aspect ratio for this part of the study (compare Figs. 3 and 4 at $R = 1$—all the curves are fairly closely bunched). With the exception of one CFRP plate ($N_L = 3$ and $c/a = d/b = 1$), failure always initiated in the first lamina at the plate centre.

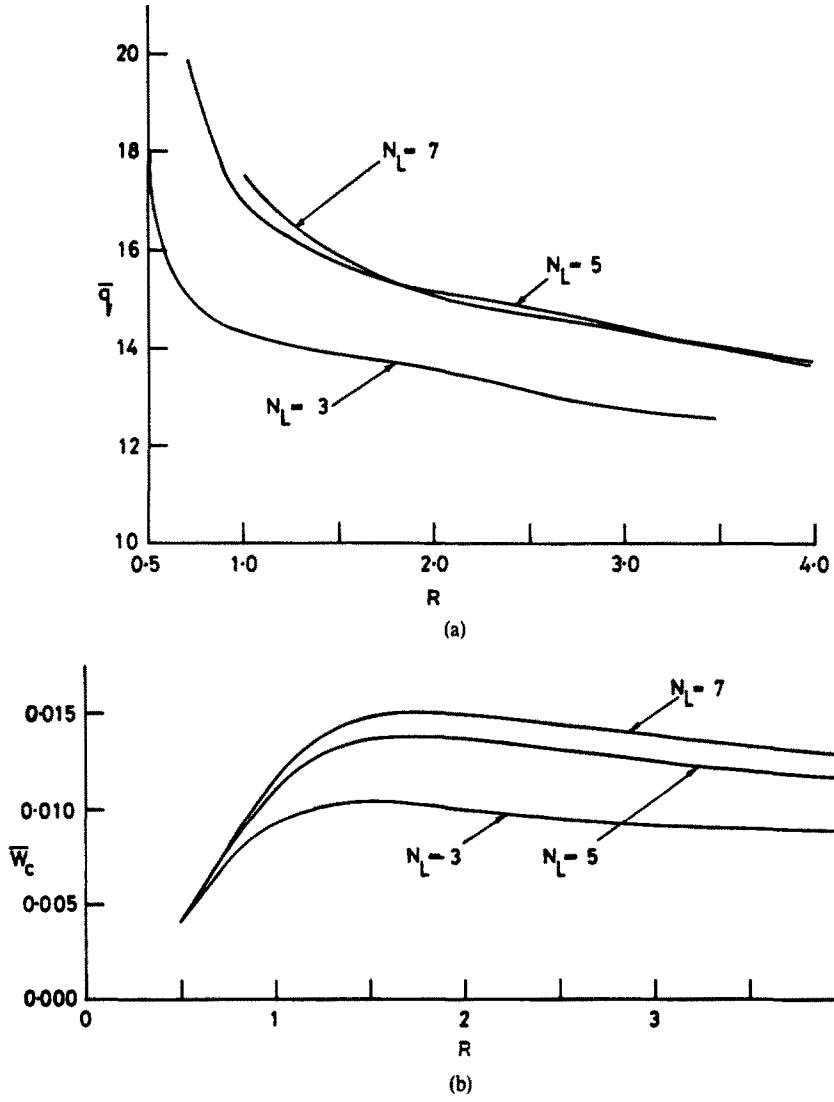

Fig. 8. Hydrostatically loaded, simply supported CFRP Cross-ply plate. (a) Initial failure load vs plate aspect ratio. (b) Corresponding plate centre deflection vs plate aspect ratio.

The final set of results of this study—those for hydrostatically loaded GFRP and CFRP plates—are presented in Figs. 7 and 8. The initial failure loads for both material types show a continuous decrease with increasing aspect ratio. In Fig. 7(a) the initial failure loads for $N_L = 7$ are significantly lower than those for $N_L = 3$ or 5 when $R > 2$. By contrast, for CFRP plates (see Fig. 8a) the initial failure loads for $N_L = 3$ are much lower than those for $N_L = 5$ or 7, which are almost indistinguishable, throughout the range of aspect ratios considered. The number of laminae in the plate therefore influences the initial failure load, but no definite pattern emerges. Under hydrostatic loading failure occurs in either the first or second lamina (along the plate centre-line) in GFRP plates and the range of aspect ratios appropriate to each is indicated against each curve of Fig. 7(a). By contrast, in similarly loaded CFRP plates failure always occurs in the first lamina.

The corresponding plate centre deflections are presented in Figs. 7(b) and 8(b) for hydrostatically loaded GFRP and CFRP plates. The deflections increase initially with increasing aspect ratio, reaching their maximum values in the range, $1.5 \leq R \leq 2.5$ and thereafter showing a moderate decrease. In addition, the CFRP plate deflections increase as N_L increases (see Fig. 8b).

5. CONCLUSIONS

An initial flexural failure study of simply supported GFRP and CFRP plates subjected to three lateral pressure distributions has been undertaken. The study has been restricted to symmetric, cross-ply lay-ups so that both types of plate exhibit flexurally orthotropic properties—the degree of orthotropy being greater in the CFRP plates.

The results of the study have been presented graphically as a set of initial failure load and corresponding plate centre deflection curves to facilitate design application. The main features of these results may be summarised as follows:

(1) Initial failure loads of uniformly loaded GFRP and CFRP plates exhibit local minima at $R \simeq 1$ and are aspect ratio independent beyond $R \simeq 2$. Their corresponding plate centre deflections are independent of N_L provided $R < 1.1$ and when $R > 2$ they tend to constant values.

(2) The uniformly loaded GFRP and CFRP results indicate that when $R > 1$ maximum strength is achieved by minimising the number of constituent lamina. Conversely, when $R < 1$ the strength may be improved by increasing the number of laminae.

(3) Initial failure loads of square plates subjected to a central, uniform, square patch load decrease with increasing patch size. The inverse situation applies in respect of the corresponding plate centre deflections. The number of laminae in the plate has practically no influence on the initial failure load or the deflection.

(4) Initial failure loads of hydrostatically loaded GFRP and CFRP plates decrease with increasing aspect ratio and the corresponding plate centre deflections exhibit maxima in the range, $1.5 \leq R \leq 2.5$.

Acknowledgements—The author wishes to record his indebtedness to the Department of Engineering for the use of its in-house computing facilities and to his father, Mr. George Turvey, for his skill in the preparation of the figures.

REFERENCES

1. S. W. Tsai, Strength characteristics of composite materials, *NASA* CR-224, (April 1965).
2. S. W. Tsai, Structural behaviour of composite materials. *NASA* CR-71 (July 1964).
3. D. Purslow, private communication, Royal Aircraft Establishment, Farnborough (1979).
4. R. M. Jones, *Mechanics of Composite Materials*, p. 249. McGraw-Hill, New York (1975).
5. S. W. Tsai, Strength theories of filamentary structures. *Fundamental Aspects of Fiber Reinforced Plastic Composites* (Edited by R. T. Schwartz and H. S. Schwartz), pp. 3–11 Wiley, New York (1968).